

Supporting Information

Edge Reconstructions of Black Phosphorene: A Global Search

Yue Liu,^a Da Li,^{a*} Tian Cui^{b,a}

^aState Key Lab of Superhard Materials, College of Physics, Jilin University, Changchun 130012, P. R. China.

^bSchool of Physical Science and Technology, Ningbo University, Ningbo 315211, P.R. China.

Figure S1. The second most stable structures of ZZ, AC and SD edges at various local phosphorus concentrations.

Figure S2. The third most stable structures of ZZ, AC and SD edges at various local phosphorus concentrations.

Figure S3. The fourth most stable structures of ZZ, AC, and SD edges at various local phosphorus concentrations.

Figure S4. The detailed planar diagram of the polygon arrangement of AC edges.

Figure S5. Edge formation energy spectra and the corresponding structures of the SD edge of black phosphorene at a local phosphorus concentration of 0.715 atoms/Å.

Figure S6. Edge formation energy spectra of the ZZ, AC, and SD edges of black phosphorene.

Figure S7. The total energy profiles of the most stable and second most stable edges at 300K and 800K during AIMD simulations.

Figure S8. Phonon spectra of the lowest energy structure.

Figure S9. Band structures of ZZ0 (pristine ZZ), ZZ2-i (ZZRC-o), ZZ2-ii (ZZRC-i), and AC4-i.

Figure S10. Band structure of the 10 most stable ZZ edges of black phosphorene ZZ nanoribbons.

Figure S11. Band structure of the 10 most stable AC edges of black phosphorene AC nanoribbons.

Figure S12. Band structure of the 10 most stable SD edges of black phosphorene SD nanoribbons.

Table S1 The edge formation energies of the zigzag edges in the database.

Table S2 The edge formation energies of the armchair edges in the database.

Table S3 The edge formation energies of the skewed diagonal edges in the database.

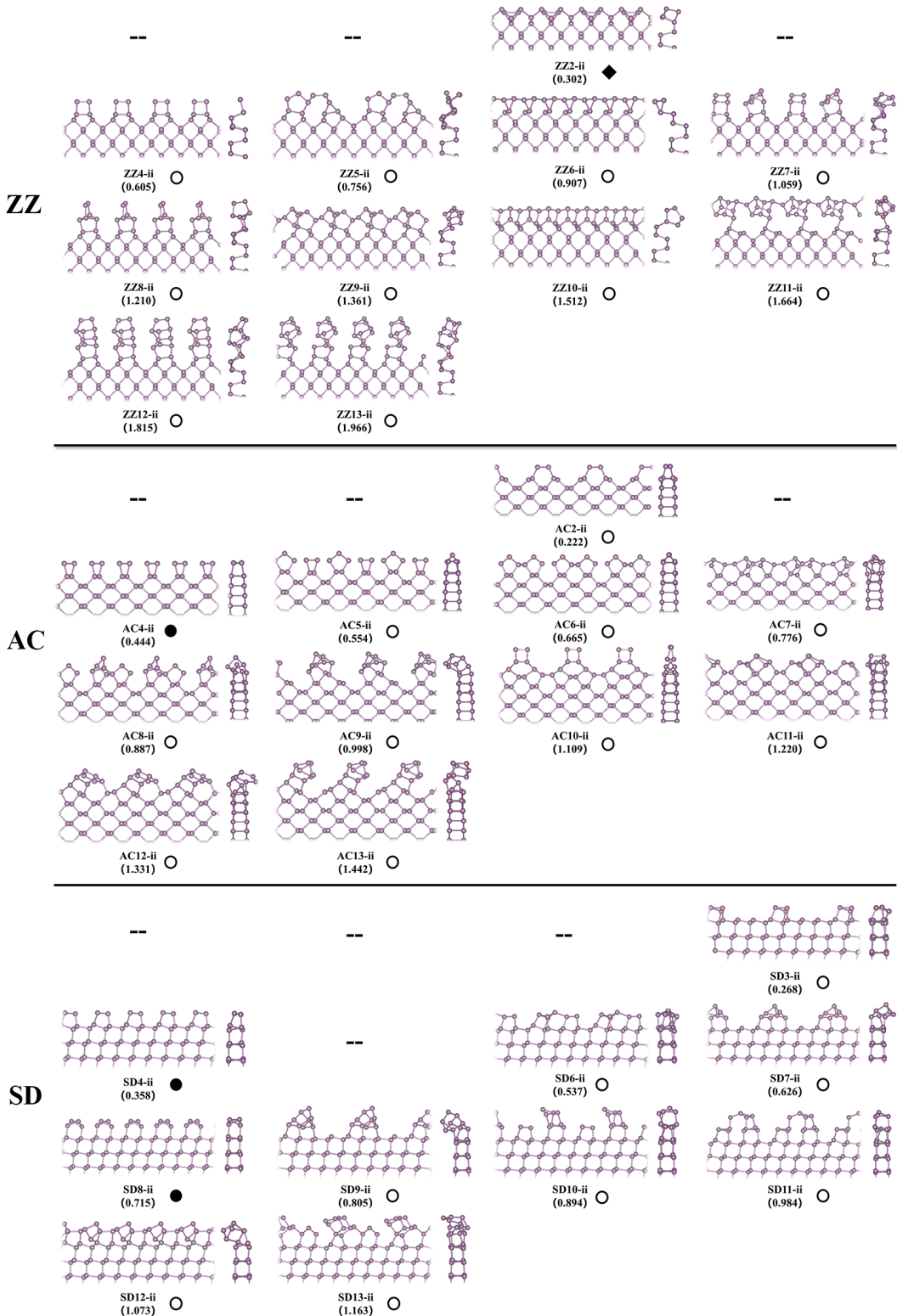


Figure S1. The second most stable structures of ZZ, AC and SD edges at various local phosphorus concentrations. The ○, ●, and ◆ shapes indicate the edges found in the current work only, in previous theoretical studies, and in previous theoretical and experimental works, respectively.

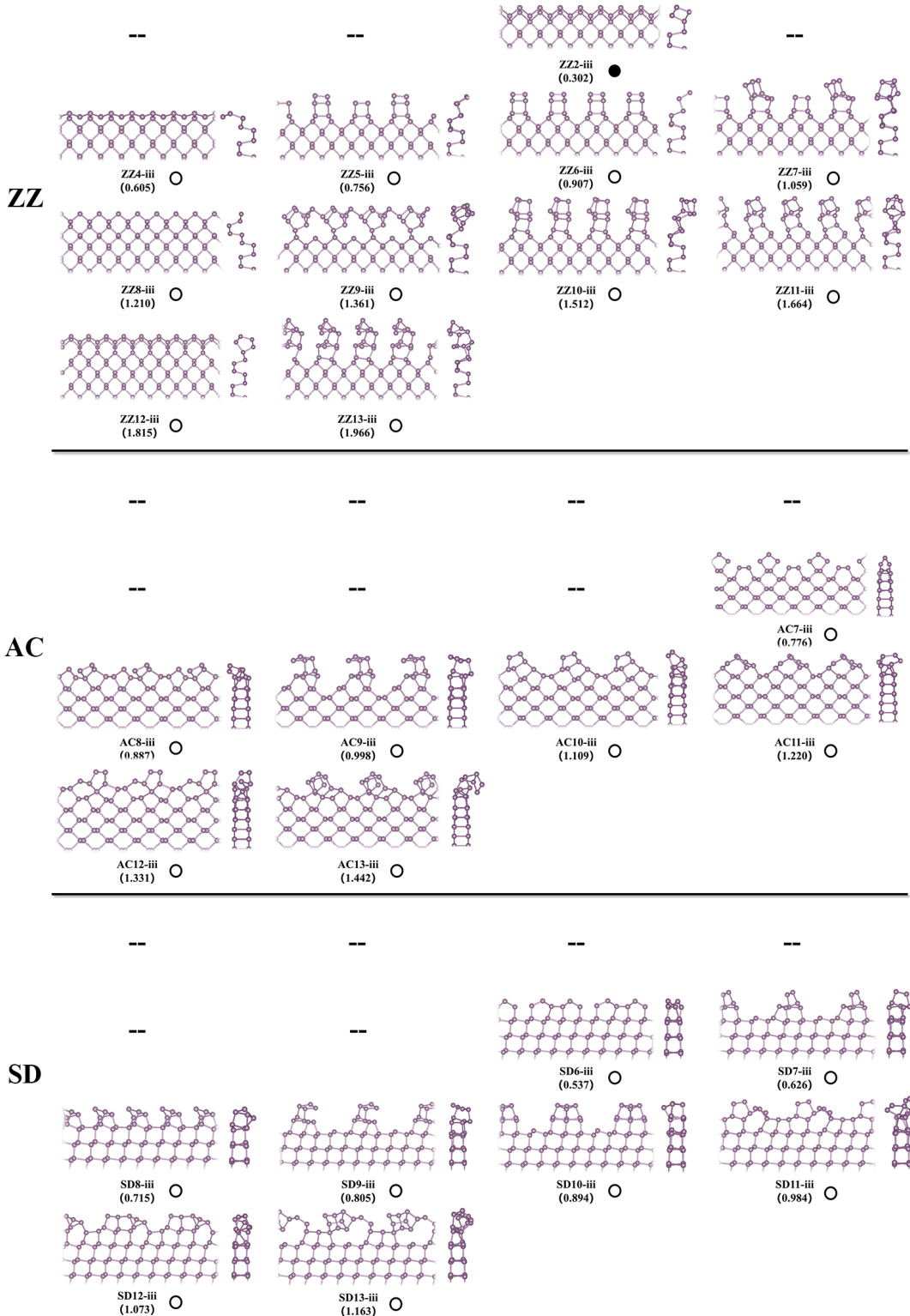


Figure S2. The third most stable structures of ZZ, AC and SD edges at various local phosphorus concentrations. The ○, ●, and ◆ shapes indicate the edges found in the current work only, in previous theoretical studies, and in previous theoretical and experimental works, respectively.

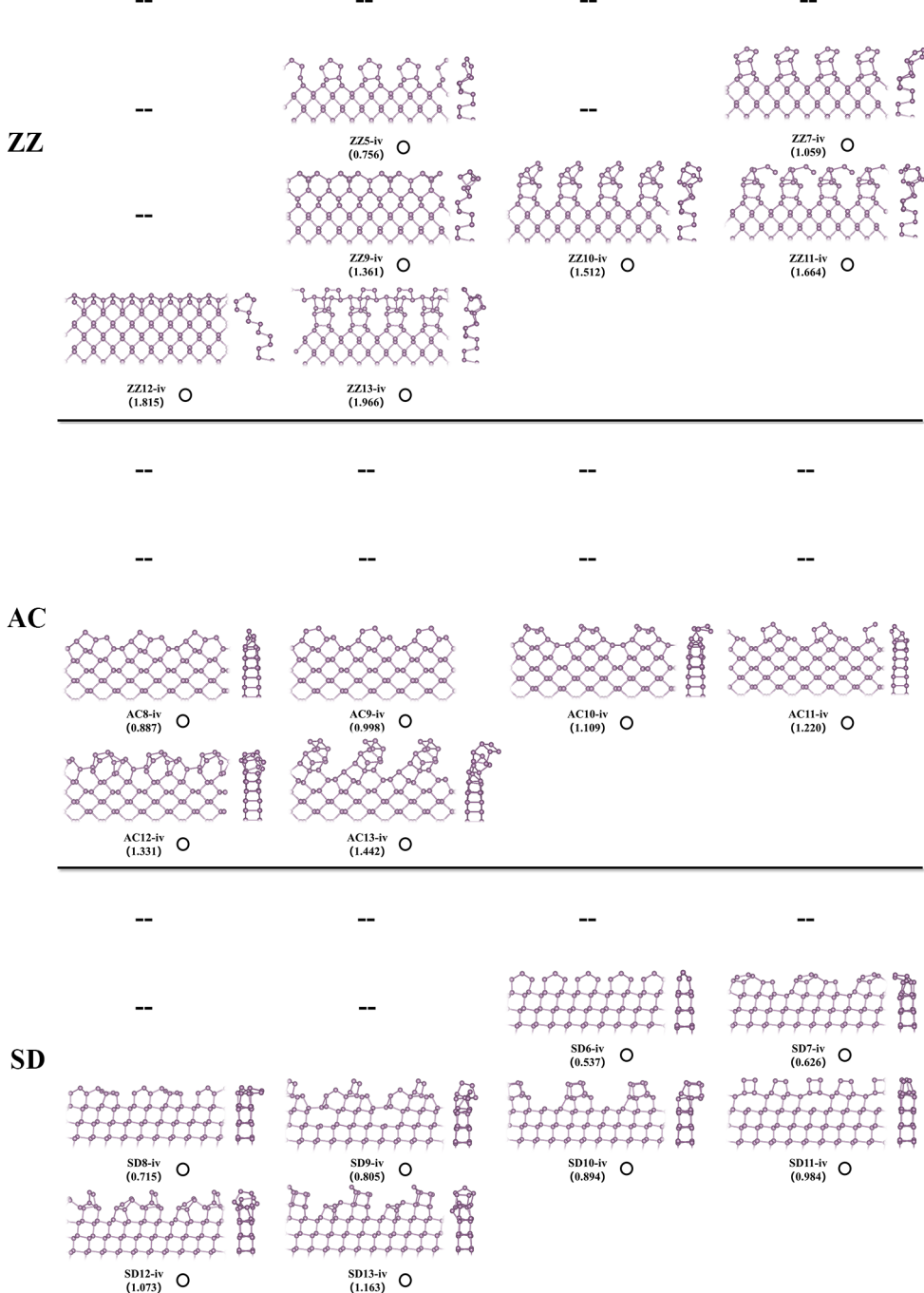


Figure S3. The fourth most stable structures of ZZ, AC, and SD edges at various local phosphorus concentrations. The ○, ●, and ◆ shapes indicate the edges found in the current work only, in previous theoretical studies, and in previous theoretical and experimental works, respectively.

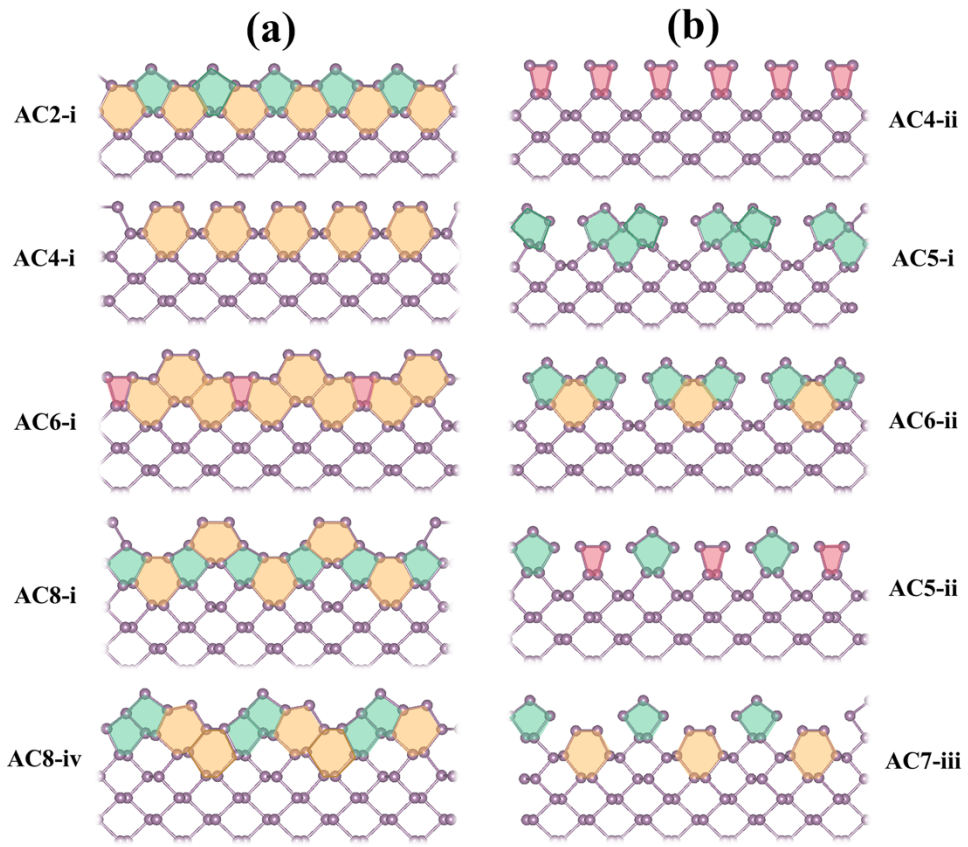


Figure S4. The detailed planar diagram of the polygon arrangement of AC edges. (a) The edges are fully occupied by polygons; (b)The edges are not fully occupied by polygons. Red, green and yellow polygons represent the quadrilateral, pentagon and hexagon, respectively.

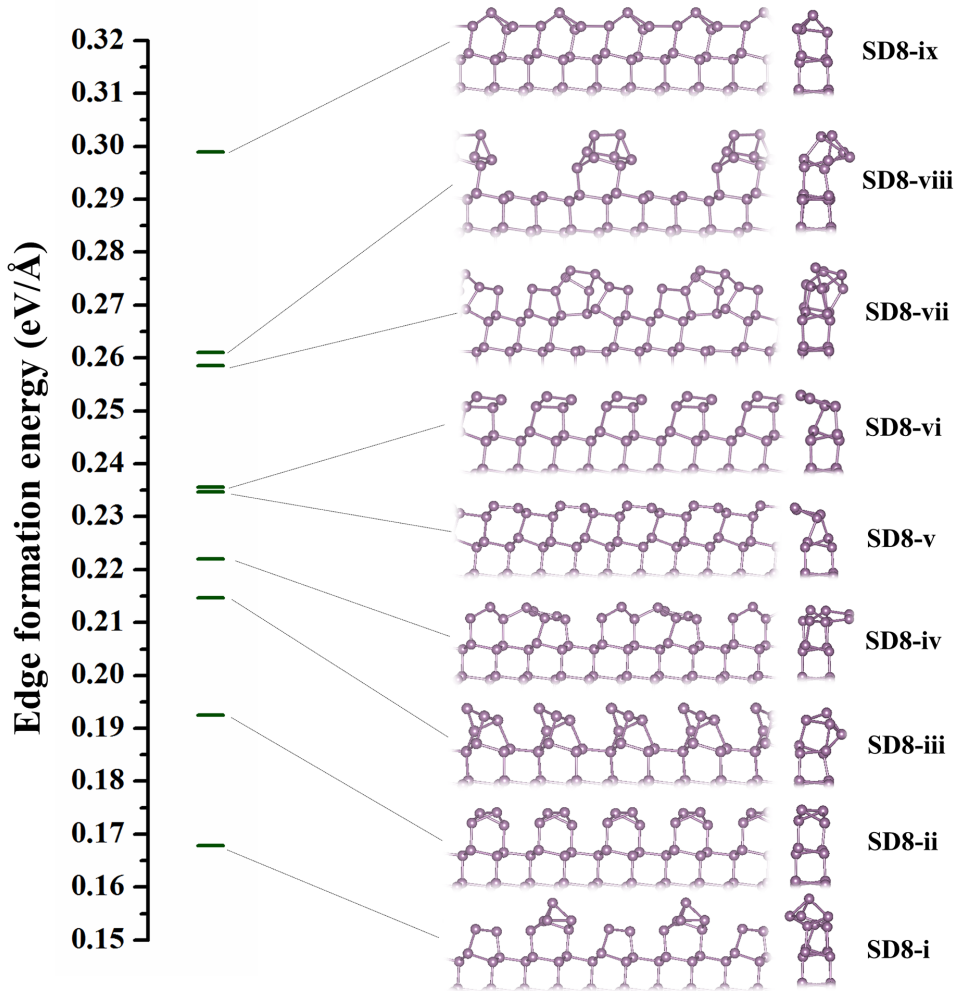


Figure S5. Edge formation energy spectra and the corresponding structures of the SD edge of black phosphorene at a local phosphorus concentration of 0.715 atoms/ \AA . The SD8-ii and SD8-ix edges have been proposed by previous theoretical work. The other seven edges are first proposed in this work.

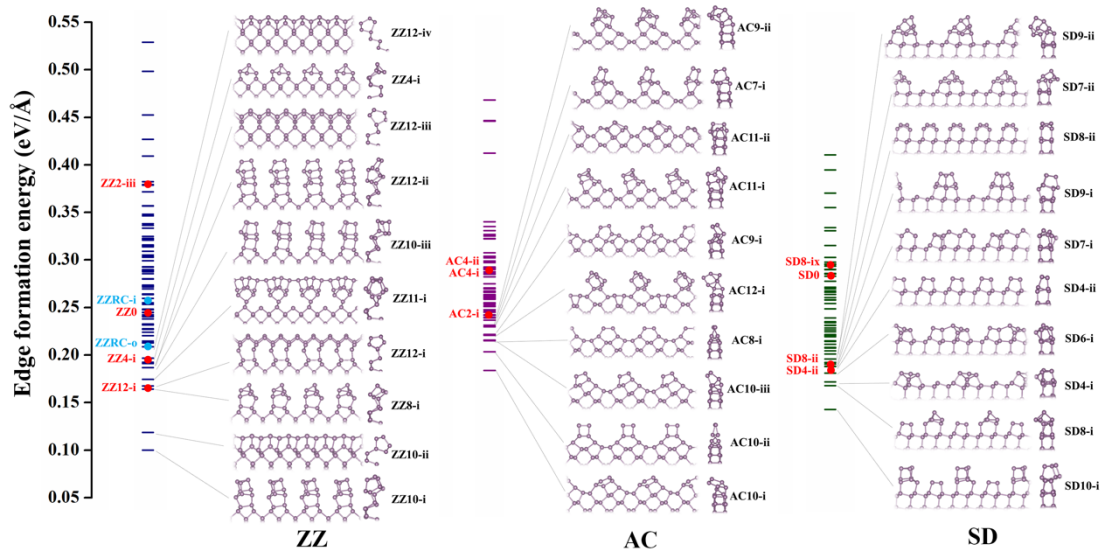


Figure S6. Edge formation energy spectra of the ZZ, AC, and SD edges of black phosphorene. The inset in each column shows the 10 most stable edges. The edge formation energies of the experimentally observed edges are highlighted by blue points; the edges energies of previous theoretically proposed edges are highlighted by red points.

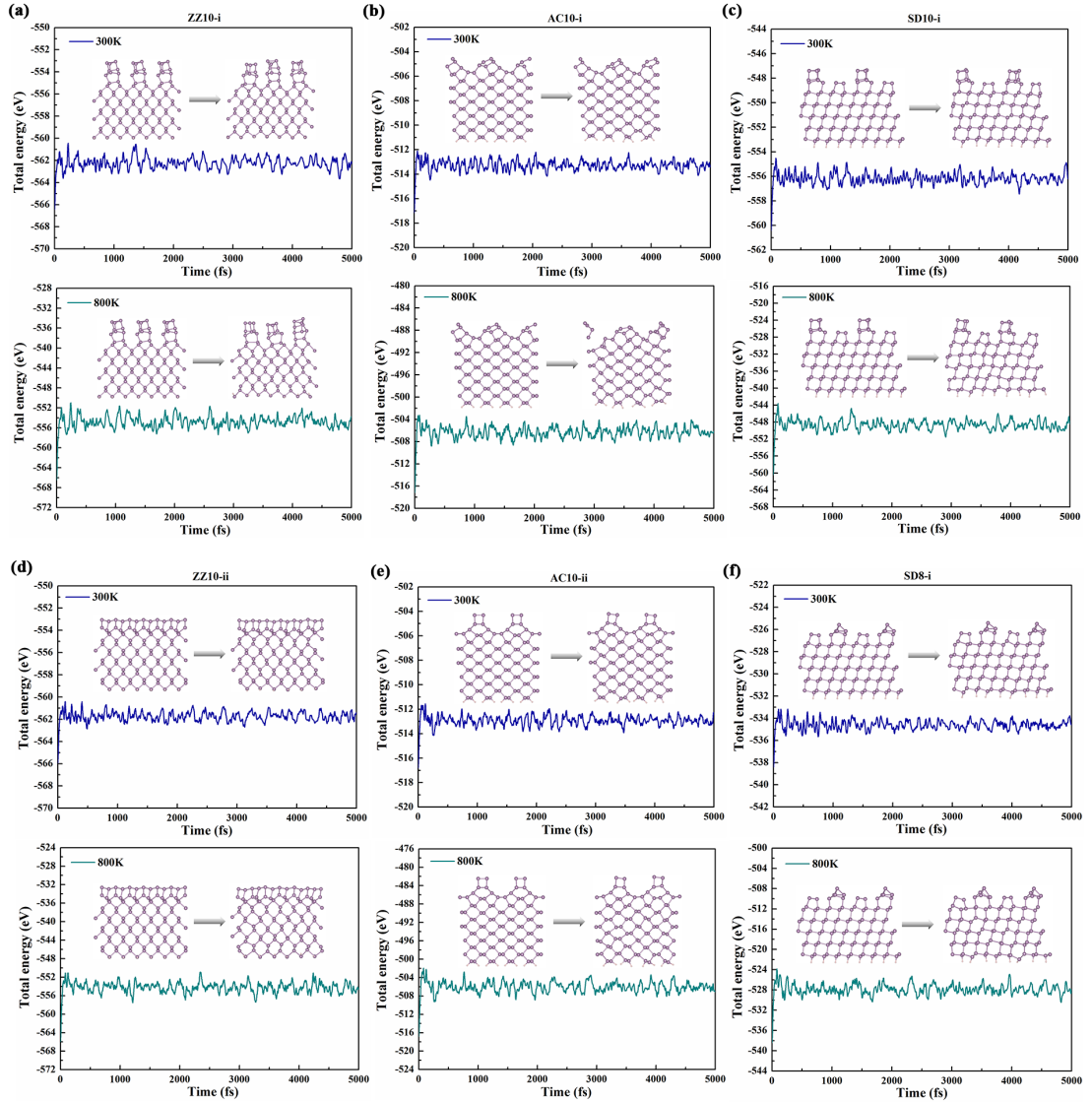


Figure S7. The total energy profiles of the most stable edges (a) ZZ10-i, (b) AC10-i and (c) SD10-i edges and second most stable edges (d) ZZ10-ii, (e) AC10-ii, (f) SD8-i at 300 K (blue line) and 800 K (green line) during AIMD simulations. Insets in each figure are structure snapshots of the AIMD simulations at 0 and 5000 fs.

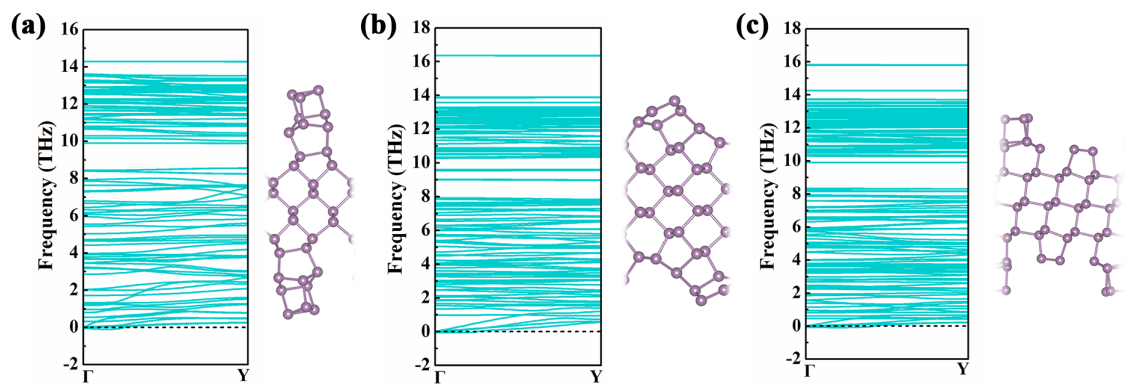


Figure S8. Phonon spectra of the lowest energy structure (a) ZZ10-i, (b) AC10-i, (c) SD10-i. The phonon spectra calculations were carried out with $1 \times 3 \times 1$ supercell using the PHONOPY code.¹

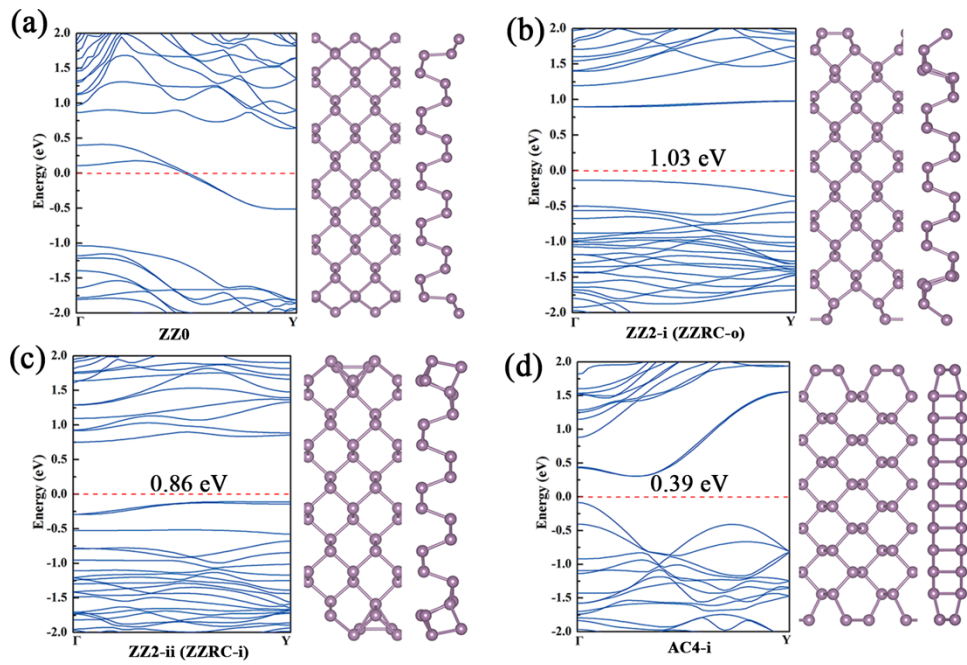


Figure S9. Band structures of (a) ZZ0 (pristine ZZ), (b) ZZ2-i (ZZRC-o), (c) ZZ2-ii (ZZRC-i), (d) AC4-i. Corresponding band gaps are directly shown in each figure.

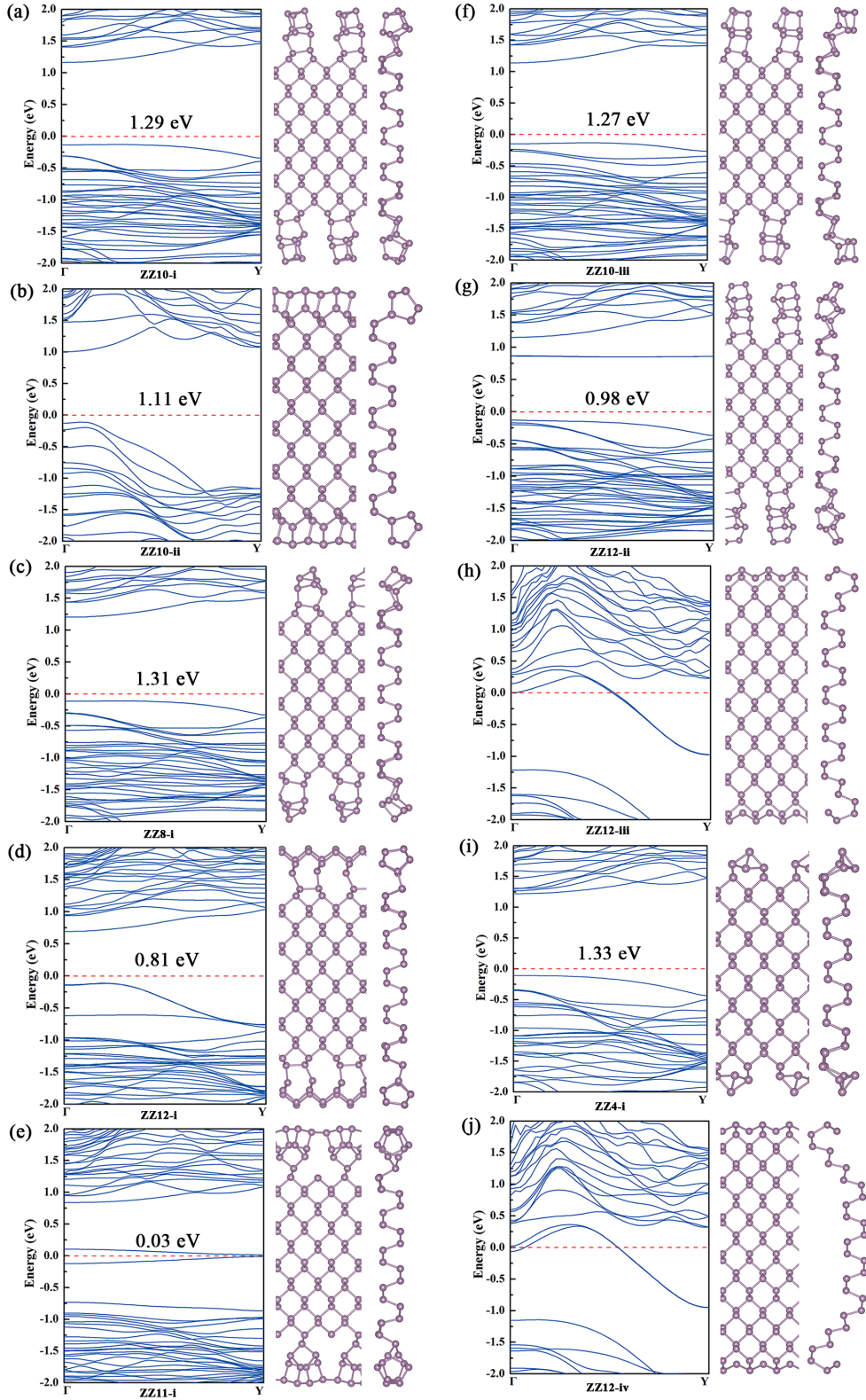


Figure S10. Band structure of the 10 most stable ZZ edges of black phosphene ZZ nanoribbons. The 7 ZZ edges (a) ZZ10-i, (b) ZZ10-ii, (c) ZZ8-i, (d) ZZ12-i, (f) ZZ10-iii, (g) ZZ12-ii and (i) ZZ4-i are semiconductors. The (e) ZZ11-i is a narrow bandgap semiconductor. The 2 edges (h) ZZ12-iii and (j) ZZ12-iv are metallic. Corresponding band gaps are directly shown in each figure.

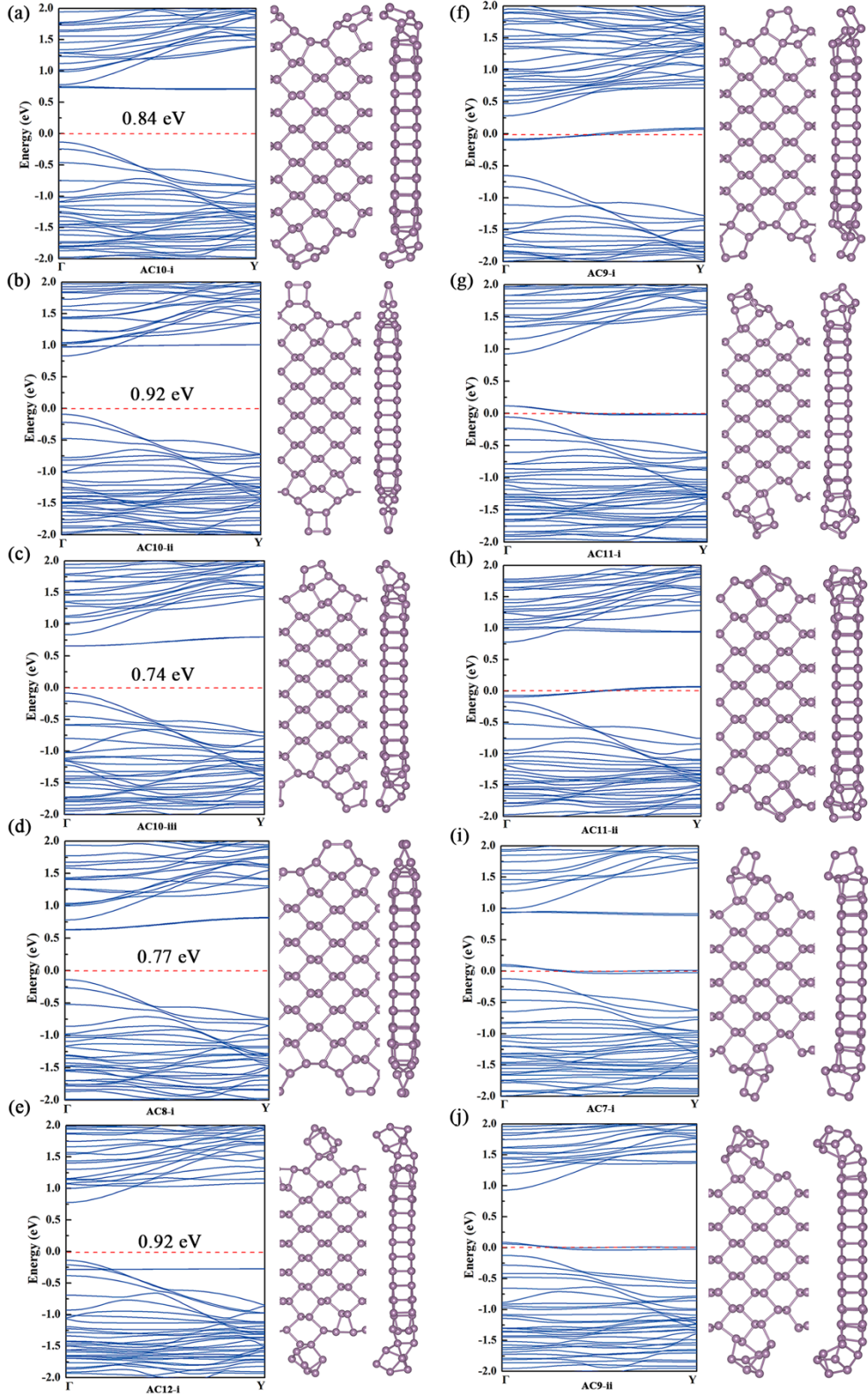


Figure S11. Band structure of the 10 most stable AC edges of black phosphorene AC nanoribbons. The 5 AC edges (a) AC10-i, (b) AC10-ii, (c) AC10-iii, (d) AC8-i and (e) AC12-i are semiconductors. The other 5 edges (f) AC9-i, (g) AC11-i, (h) AC11-ii, (i) AC7-i and (j) AC9-ii are metallic. Corresponding band gaps are directly shown in each figure.

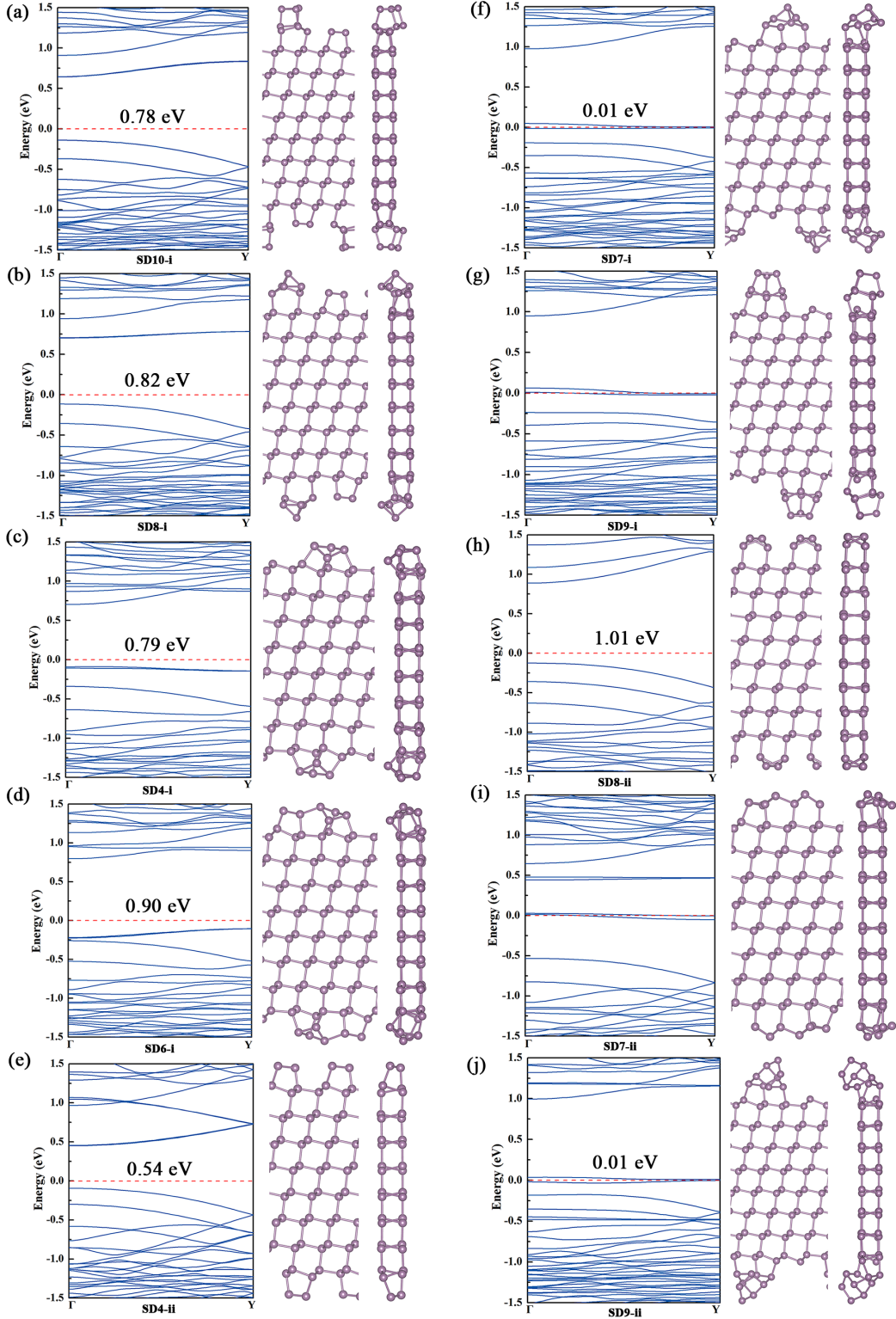


Figure S12. Band structure of the 10 most stable SD edges of black phosphorene SD nanoribbons. The 6 SD edges (a) SD10-i, (b) SD8-i, (c) SD4-i, (d) SD6-i, (e) SD4-ii, and (h) SD8-ii are semiconductors. The 2 edges (f) SD7-i and (j) SD9-ii are narrow bandgap semiconductors. The other 2 edges (g) SD9-i and (i) SD7-ii are metallic. Corresponding band gaps are directly shown in each figure.

Table S1 The edge formation energies of the zigzag edges in the database.

ZZx-i	Edge energy (eV/Å)	ZZx-ii	Edge energy (eV/Å)	ZZx-iii	Edge energy (eV/Å)	ZZx-iv	Edge energy (eV/Å)
ZZ-0	0.24081	--	--	--	--	--	--
ZZ1-i	0.24460	--	--	--	--	--	--
ZZ2-i	0.21269	ZZ2-ii	0.27243	ZZ2-iii	0.38241	--	--
ZZ3-i	0.23174	--	--	--	--	--	--
ZZ4-i	0.19665	ZZ4-ii	0.26411	ZZ4-iii	0.31586	--	--
ZZ5-i	0.24233	ZZ5-ii	0.25972	ZZ5-iii	0.28543	ZZ5-iv	0.32097
ZZ6-i	0.22397	ZZ6-ii	0.23549	ZZ6-iii	0.31387	--	--
ZZ7-i	0.25390	ZZ7-ii	0.27159	ZZ7-iii	0.28029	ZZ7-iv	0.35667
ZZ8-i	0.16414	ZZ8-ii	0.28755	ZZ8-iii	0.37847	--	--
ZZ9-i	0.21450	ZZ9-ii	0.22705	ZZ9-iii	0.23779	ZZ9-iv	0.25503
ZZ10-i	0.10001	ZZ10-ii	0.11861	ZZ10-iii	0.18682	ZZ10-iv	0.22781
ZZ11-i	0.17442	ZZ11-ii	0.20149	ZZ11-iii	0.24823	ZZ11-iv	0.30283
ZZ12-i	0.16747	ZZ12-ii	0.19197	ZZ12-iii	0.19227	ZZ12-iv	0.20856
ZZ13-i	0.22025	ZZ13-ii	0.24021	ZZ13-iii	0.27984	ZZ13-iv	0.29239

Table S2 The edge formation energies of the armchair edges in the database.

ACx-i	Edge energy (eV/Å)	ACx-ii	Edge energy (eV/Å)	ACx-iii	Edge energy (eV/Å)	ACx-iv	Edge energy (eV/Å)
AC-0	0.35756	--	--	--	--	--	--
AC1-i	0.31298	--	--	--	--	--	--
AC2-i	0.26186	AC2-ii	0.33461	--	--	--	--
AC3-i	0.27894	--	--	--	--	--	--
AC4-i	0.29690	AC4-ii	0.30090	--	--	--	--
AC5-i	0.27007	AC5-ii	0.27539	--	--	--	--
AC6-i	0.24911	AC6-ii	0.25255	--	--	--	--
AC7-i	0.24601	AC7-ii	0.27129	AC7-iii	0.30833	--	--
AC8-i	0.22505	AC8-ii	0.25155	AC8-iii	0.25488	AC8-iv	0.27262
AC9-i	0.23115	AC9-ii	0.24822	AC9-iii	0.27628	AC9-iv	0.27916
AC10-i	0.19300	AC10-ii	0.21274	AC10-iii	0.22438	AC10-iv	0.27018
AC11-i	0.23913	AC11-ii	0.24057	AC11-iii	0.26164	AC11-iv	0.26940
AC12-i	0.23015	AC12-ii	0.25421	AC12-iii	0.28005	AC12-iv	0.29147
AC13-i	0.24867	AC13-ii	0.25665	AC13-iii	0.29679	AC13-iv	0.30677

Table S3 The edge formation energies of the skewed diagonal edges in the database.

SDx-i	Edge energy (eV/Å)	SDx-ii	Edge energy (eV/Å)	SDx-iii	Edge energy (eV/Å)	SDx-iv	Edge energy (eV/Å)
SD-0	0.28279	--	--	--	--	--	--
SD1-i	0.29078	--	--	--	--	--	--
SD2-i	0.23165	--	--	--	--	--	--
SD3-i	0.21541	SD3-ii	0.22131	--	--	--	--
SD4-i	0.17171	SD4-ii	0.18794	--	--	--	--
SD5-i	0.20493	--	--	--	--	--	--
SD6-i	0.18112	SD6-ii	0.20469	SD6-iii	0.21983	SD6-iv	0.25903
SD7-i	0.18830	SD7-ii	0.19618	SD7-iii	0.20767	SD7-iv	0.20847
SD8-i	0.16783	SD8-ii	0.19245	SD8-iii	0.21470	SD8-iv	0.22207
SD9-i	0.19093	SD9-ii	0.20142	SD9-iii	0.23958	SD9-iv	0.27220
SD10-i	0.14238	SD10-ii	0.22705	SD10-iii	0.25497	SD10-iv	0.26464
SD11-i	0.22066	SD11-ii	0.24928	SD11-iii	0.26453	SD11-iv	0.28632
SD12-i	0.21159	SD12-ii	0.22516	SD12-iii	0.22901	SD12-iv	0.23187
SD13-i	0.25493	SD13-ii	0.27865	SD13-iii	0.29450	SD13-iv	0.29622

References

1. A. Togo and I. Tanaka, *Scripta Materialia*, 2015, **108**, 1-5.